International Journal of analytical and Numerical Methods in Mechanical Design
Vol 3., Issue 1 Winter & Spring, 2024, 25-32

Optimal Torque Allocation for Energy Efficiency Enhancement in In-Wheel Motor Drive Electric Vehicles

Majid Majidi*
Department of Mechanical Engineering, Qazvin Branch, Islamic Azad University, Qazvin, Iran

Received 15 March 2024, Accepted 25 May 2024

Abstract

This paper proposes a multi-level hierarchical control method to enhance the stability of electric vehicles (EVs) equipped with four independent in-wheel motors. At the high level, a sliding mode controller determines the total desired force and yaw moment. At the low level, an optimal energy-efficient control allocation scheme distributes torques among the four in-wheel motors. This research investigates both handling performance and energy efficiency, evaluated through a co-simulation approach using MATLAB/Simulink and CarSim. A torque distribution algorithm, based on energy efficiency optimization, is applied to control the EV during lane change maneuvers, both with and without the proposed controller. Simulation results demonstrate that the proposed torque control system and distribution algorithm effectively maintain vehicle stability, reduce energy consumption, and accurately track the desired yaw rate and longitudinal velocity during these maneuvers.

Keywords: control allocation, EV, sliding mode control, torque distribution, stability enhancement

1. Introduction

Environmental concerns and the increasing focus on sustainable transportation have positioned electric vehicles (EVs), often referred to as zero-emission vehicles, at the forefront of global mobility solutions. However, given the current limitations in battery energy density, effective energy management is crucial for extending the driving range and enhancing the overall efficiency of EVs. Advanced drive technologies and innovative control strategies are essential to overcoming these challenges and fully leveraging the potential of EV powertrains [1].

A promising approach involves integrating in-wheel electric motors, which enable independent control of driving and braking torques at each wheel. This configuration not only enhances energy management but also provides significant advantages for vehicle stability. In lateral dynamics control, yaw rate is typically considered the primary control variable, while the vehicle sideslip angle is constrained by regulating its angular velocity. To maintain the desired dynamic performance, a corrective yaw moment-often generated via direct yaw moment control (DYC) systems-is employed to ensure that the yaw rate tracks its target value, thereby keeping the sideslip angle within safe limits. Conventional DYC systems are generally classified into two main categories: differential braking systems (DBS) and torque vectoring (TV) systems. The independent torque control capability of in-wheel motors makes them particularly well-suited for implementing such systems [2].

Extensive research has been conducted on torque distribution and energy-efficient control strategies for EVs. For example, Mashadi and Majidi [3] demonstrated the benefits of using rear-wheel-embedded motors to generate a direct yaw moment, addressing the limitations of conventional electronic stability control (ESC) systems. In [4], a control algorithm was developed to optimize driving efficiency while considering tire slip and cornering dynamics, employing a fuzzy controller to coordinate torque distribution strategies for improved stability and energy efficiency.

Other studies have made notable contributions in this field. Dizqah et al. [5] developed an analytical framework to determine the necessary torque range, showing that adjusting the torque on one side of the vehicle can reduce energy consumption by up to 5% compared to single-axle configurations. Koehler et al. [6] applied optimization techniques to determine the ideal yaw rate and slip angle during cornering, achieving approximately a 10% reduction in energy consumption. Similarly, Filippis et al. [7] and Sun et al. [8] illustrated that fine-tuned torque vectoring control can further enhance energy savings. Additional research efforts have leveraged model predictive control (MPC) [9-12], deep reinforcement learning [13], and multi-objective online optimization

Corresponding Author: m_majidi@qiau.ac.ir

[14] to simultaneously address vehicle stability and energy efficiency challenges in EVs.

Building on these advances, this paper introduces a novel hierarchical control strategy for an EV equipped with four independent in-wheel motors. At the high level, a sliding mode controller (SMC) computes the total longitudinal force and yaw moment required to accurately track the desired yaw rate and velocity profiles during critical maneuvers. At the low level, an optimal control allocation scheme distributes the computed torques among the four in-wheel motors. This approach minimizes energy consumption while ensuring that the dynamic performance targets are met. Simulation results confirm that the proposed control framework enhances vehicle stability and reduces energy consumption during severe driving maneuvers.

The remainder of this paper is organized as follows. Section II describes the vehicle model and the overall control architecture. Section III details the design of the sliding mode controller and the optimal torque allocation scheme. Section IV presents simulation results and discusses the performance of the proposed strategy. Finally, Section V concludes the paper and outlines future research directions.

2. Vehicle Modeing

Dynamic control of a vehicle relies on accurate mathematical modeling of its dynamic behavior. Vehicle modeling is essential for simulating various driving conditions and predicting the vehicle response to control inputs. Extensive research in automotive dynamics has focused on identifying critical parameters and variables-such as mass distribution, tire forces, and aerodynamic effects-that influence vehicle motion and stability.

CarSim is a widely used and powerful vehicle dynamics simulation software, offering computational efficiency that is three to six times faster than real-time simulations. It enables comprehensive analysis of vehicle responses to driver inputs, road conditions, and aerodynamic effects. CarSim is commonly utilized for evaluating key performance metrics, including handling stability, ride comfort, dynamic characteristics, braking efficiency, and overall energy consumption. Additionally, it allows developers to customize simulation environments, define control system parameters, and modify characteristic files to meet specific research requirements.

In this study, a four-in-wheel motor electric vehicle (EV) model is developed using CarSim to simulate its dynamic behavior. Since the default CarSim vehicle models are designed for traditional internal combustion engine (ICE) vehicles, modifications are required to accurately represent the distributed drive system of an in-wheel motor EV. This involves removing conventional drivetrain components, such as the engine, gearbox, and differential, as illustrated in Fig 1. Furthermore, to enable co-simulation with MATLAB/Simulink, input and output interfaces for the CarSim model are defined. A custom drive torque output model is integrated into the simulation, replacing the conventional transmission system to accurately represent the distributed drive configuration of the EV.

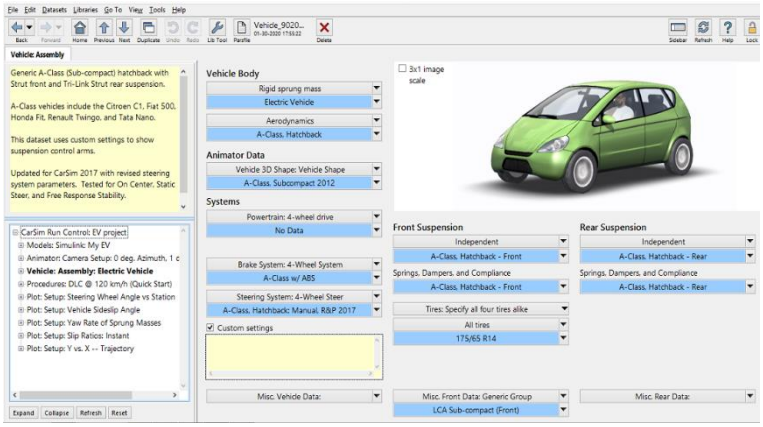

Fig 1. Modification of CarSim vehicle model for in-wheel motor EV

2.1 Electric Motors

Permanent Magnet Synchronous Motors (PMSMs) have gained significant attention for in-wheel applications due to their high efficiency and precise torque control capabilities. Typically, drive motors positioned within the wheel assembly contribute to the vehicle unsprung mass. However, most commercially available electric motors are too heavy for direct integration into drive wheels. Therefore, two critical factors for in-wheel motor applications are low mass and a high torque-to-mass ratio.

One of the key advantages of PMSMs is that their rotors contain permanent magnets, eliminating copper losses and magnetizing currents typically found in conventional DC motors. Additionally, PMSMs allow for direct and efficient torque control, which is highly beneficial for electric vehicles (EVs) with in-wheel motors. Given that the motor's dynamic response is significantly faster than that of the wheel dynamics, the motor and its controller can be approximated as a first-order delay system, represented by the following transfer function:

$$\frac{T_m}{T_c} = \frac{1}{(L_s/R_s)s+1} \quad (1)$$

where R_s and L_s are the motor winding resistance and inductance, respectively, T_c is the commanded torque from the torque distribution controller, and T_m is the actual torque applied to the wheel.

In this study, the selected PMSM has a maximum speed of 6000 rpm, a peak torque of 128 Nm, and a maximum power output of 25 kW, ensuring it meets the performance requirements of the EV. As illustrated in Fig 2, the driving and braking torque limitations for each in-wheel motor are functions of motor speed. Given the high-speed characteristics of the selected motor, a speed reduction mechanism with a reduction ratio of 2 is implemented to optimize torque delivery and enhance vehicle performance.

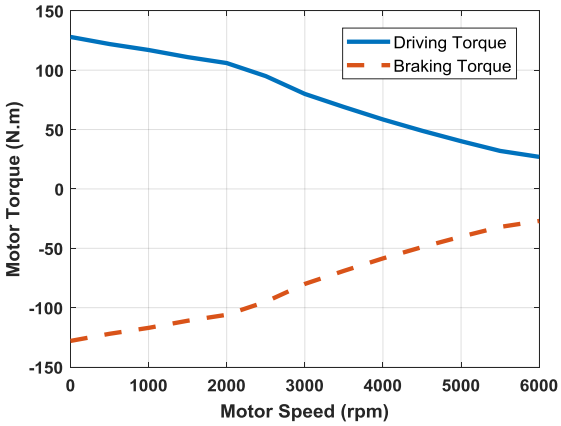

Fig 2. Torque-speed characteristics of the in-wheel motor

3. Controller Design

To enhance vehicle handling and stability, a multi-layered control system has been developed, consisting of two hierarchical layers, as illustrated in Fig 3. The high-level controller generates the total longitudinal force and yaw moment based on the driver's input commands, as well as yaw rate and longitudinal velocity signals from the vehicle. These control inputs are then transmitted to the low-level controller, which employs a torque allocation algorithm to distribute the optimal torque among the in-wheel motors, ensuring energy-efficient actuation of the vehicle.

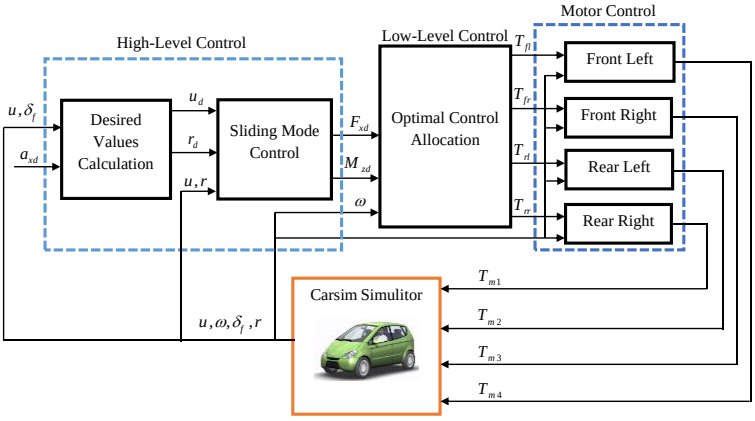

Fig 3. The proposed control structure

3.1 Desired Values Generation

The high-level controller aims to minimize the discrepancy between the actual and desired vehicle responses during maneuvers. One of the critical aspects of controller design is the accurate determination of the desired vehicle response. A two-degree-of-freedom model is utilized to establish the reference yaw rate and longitudinal velocity, defined as follows:

$$v_{xd} = v_{x0} + \int_0^t a_{xd}(\tau)\,d\tau \quad (2)$$

$$\dot{\psi}_d = \frac{v_x \delta_f}{L + K_{us} v_x^2} \quad (3)$$

Where v_{xd} and ψ_d are desired longitudinal velocity and yaw rate, respectively. K_{us} is the understeer gradient is determined by coefficients of the tire cornering stiffness at different vertical loads and road conditions, and δ_f is the front wheel angle. L is the vehicle wheelbase. v_{x0} is initial longitudinal velocity and a_{xd} represents the longitudinal acceleration based on the driver's input.

3.2 High-Level Controller Design

Since EVs operate in non-linear conditions with varying parameters such as vehicle mass, tire properties, and road friction, SMC is adopted for the high-level controller. This method ensures robust control of longitudinal and lateral vehicle dynamics, enabling the actual vehicle states to follow the desired ones. The vehicle longitudinal and yaw motion equations are simplified as:

$$\begin{cases} \dot{v}_x = \frac{1}{m}(F_{xd} - 0.5 C_d A_f \rho_a v_x^2) \\ \ddot{\psi} = \frac{1}{I_z} M_{zd} \end{cases} \quad (4)$$

Where v_x, $\dot{\psi}$, are longitudinal velocity and yaw rate of the vehicle, respectively. A_f, and C_d , and ρ_a are front surface area of the vehicle, drag coefficient, and air density, respectively. m and I_z are mass of the vehicle and moment of inertia about the vertical axis of the vehicle. F_{xd} and M_{zd} are desired driving force and yaw moment. The sliding mode surfaces for longitudinal and yaw motions are defined as:

$$\begin{cases} S_v = v_x - v_{xd} \\ S_\psi = \dot{\psi} - \dot{\psi}_d \end{cases} \quad (5)$$

The sliding mode control objective is to reach and remain in the sliding surface such that $\dot{S} = 0$ based on equation (5). So, the control laws are directly derived from the sliding surfaces [3]. To have better control performance regarding the chattering phenomenon, the saturation function instead of the sign function is adopted in the process of control design, which is given by:

$$\begin{cases} \dot{s}_i = -k_i \, \text{sat}(\frac{s_i}{\phi_i}) \qquad \forall i \in \{v, \psi\} \\ \text{sat}(\frac{s_i}{\phi_i}) = \begin{cases} \frac{s_i}{\phi_i} & if \ |s_i| < \phi_i \\ \text{sgn}(\frac{s_i}{\phi_i}) & if \ |s_i| \geq \phi_i \end{cases} \end{cases} \quad (6)$$

The coefficient k_i is a positive constant determining the approaching rate of the system state on the sliding surface, the coefficient ϕ_i is used to smooth the control discontinuity in the law of sliding mode and also determines the tracking errors. The larger the value, the less the chattering, but the convergence rate of the system is slower. According to the principle of SMC, the control laws are ultimately given by:

$$\begin{cases} F_{xd} = m\,(a_{xd} - k_v \, \text{sat}(\frac{s_v}{\phi_v})) + \frac{1}{2} C_D A_f \rho_a v_x^2 \\ M_{zd} = I_z (\frac{a_{xd}(L - K_g u^2)\delta_f}{(L + K_g u^2)^2}) - k_\psi \, \text{sat}(\frac{s_\psi}{\phi_\psi})) \end{cases} \quad (7)$$

where F_{xd} and M_{zd} are obtained to pursue the best tracking performance; meanwhile, they act as inputs of the low-level controller, which generates the desired driving/braking torque commands for the four electric motor controllers.

3.3 Low-Level Controller Design

The lower-level controller is responsible for applying the corrective yaw moment and total longitudinal force generated by the upper-level controller to the vehicle. Its primary task, formulated as an optimal control allocation problem, is to distribute the required wheel torques based on a torque distribution algorithm. The computed torques serve as reference inputs for the electric motor controllers of each wheel, which then apply the necessary driving or braking torque to achieve the desired vehicle response.

Since the number of actuators (four in-wheel motors) exceeds the number of controlled states (longitudinal velocity and yaw rate), the electric vehicle (EV) is an over-actuated system. The control allocation algorithm distributes the command torques among the four in-wheel motors to achieve energy-efficient actuation while ensuring stability. The proposed torque allocation algorithm optimally assigns torques based on energy consumption minimization, ensuring that the total longitudinal force and yaw moment determined by the upper-level controller are correctly implemented.

For small steering angles, the total longitudinal force and yaw moment can be expressed as:

$$F_{xd} = F_{x-fl} + F_{x-fr} + F_{x-rl} + F_{x-rr} \quad (8)$$

$$M_{zd} = (F_{x-fr} - F_{x-fl})\frac{t_f}{2} + (F_{x-rr} - F_{x-rl})\frac{t_r}{2} \quad (9)$$

These equations serve as equality constraints in the energy consumption optimization problem described in the following section.

3.3.1 Torque distribution algorithm based on energy consumption optimization

This section presents an energy-efficient torque allocation strategy that minimizes electric motor power consumption while satisfying the equality constraints (8) and (9). The optimization ensures that the driving torques are allocated such that:

- The individual wheel forces remain within the maximum allowable motor torque and the maximum available road adhesion force, given by the product of the tire vertical force and the tire-road friction coefficient.
- Load transfer effects during acceleration and deceleration are considered, as vertical loads shift between the front and rear wheels, affecting traction availability.

Thus, the problem is formulated as a nonlinear optimization model, assuming that all four in-wheel motors have identical efficiency characteristics. The instantaneous power consumption of each motor is expressed as a function of the wheel torques:

$$P_c(T_m) = \begin{cases} \frac{T_m \omega}{\eta_m(\omega, T_m)} & if \quad T_m > 0 \\ T_m \omega \, \eta_g(\omega, T_m) & if \quad T_m < 0 \end{cases} \quad (10)$$

where η_m represents the electric motor efficiency, which differs in motor mode and generator mode. Electric motor efficiency contour of the selected PMSM is shown in Fig 4. The efficiency in generator mode can be derived from the efficiency map of the permanent magnet synchronous motor (PMSM) by assuming equal power losses in both modes:

$$P_{loss,m} = P_{loss,g} \Rightarrow T_m\omega(\frac{1}{\eta_m}-1) = T_m\omega(1-\eta_g) \Rightarrow \eta_g = 2-\frac{1}{\eta_m} \quad (11)$$

Thus, the cost function for energy optimization is formulated as:

$$J = \min \sum_{i=fl,fr,rl,rr} P_{ci}(T_{mi}) \quad (12)$$

The equality constraints ensure that the control torques satisfy the upper-level controller requirements:

$$F_{xd} = \frac{n_g}{r_w}(T_{m-fl}+T_{m-fr}+T_{m-rl}+T_{m-rr}) \quad (13)$$

$$M_{zd} = \frac{n_g}{r_w}[\frac{t_f}{2}(T_{m-fr}-T_{m-fl})+\frac{t_r}{2}(T_{m-rr}-T_{m-rl})] \quad (14)$$

where r_w is the wheel radius, n_g is a reduction ratio. t_f and t_r are the front and rear track widths. The inequality constraints include:

1. Motor Torque Limits

$$-T_{m\_i\_\max}(\omega) \le T_{m\_i} \le T_{m\_i\_\max}(\omega) \quad (15)$$

where $T_{m\_i\_\max}$ is the maximum allowable motor torque, which varies with motor speed ω_i.

2. Road Adhesion Limits

The vertical load on each wheel is determined as:

$$\begin{aligned} F_{z-fl} &= \frac{mgb}{2L}-\frac{ma_xh_g}{2L}-\frac{mb}{L}\frac{a_yh_g}{t_f} \\ F_{z-fr} &= \frac{mgb}{2L}-\frac{ma_xh_g}{2L}+\frac{mb}{L}\frac{a_yh_g}{t_f} \\ F_{z-rl} &= \frac{mga}{2L}+\frac{ma_xh_g}{2L}-\frac{ma}{L}\frac{a_yh_g}{t_r} \\ F_{z-rr} &= \frac{mga}{2L}+\frac{ma_xh_g}{2L}+\frac{ma}{L}\frac{a_yh_g}{t_r} \end{aligned} \quad (16)$$

where F_{z-i} is the vertical tire force, a_x and a_y are the vehicle longitudinal and lateral acceleration, h_g is the vehicle CG height, a and b are the distances from vehicle CG to the front and rear axles. So, the limitation of road adhesion force can be expressed as:

$$n_g|T_{m-i}| \le \mu F_{z-i}r_w \quad (17)$$

The final optimization problem is solved using the Sequential Quadratic Programming (SQP) method in MATLAB *fmincon* function.

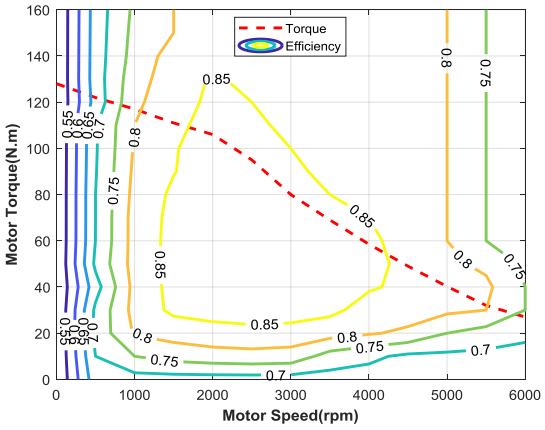

Fig 4. Electric motor efficiency contour

3.3.2 Torque distribution algorithm based on dynamic load distribution

Due to dynamic weight transfer from longitudinal and lateral accelerations, the vertical loads on the tires vary during acceleration, braking, and cornering. Since the maximum longitudinal force a tire can generate depends on its vertical load, the torque allocation strategy should consider dynamic load distribution.

The front-to-rear vertical load ratios are defined as:

$$\frac{F_{x-fl}}{F_{x-rl}} = \frac{F_{z-fl}}{F_{z-rl}} = \rho_L \qquad \frac{F_{x-fr}}{F_{x-rr}} = \frac{F_{z-fr}}{F_{z-rr}} = \rho_R \quad (18)$$

where ρ_R and ρ_L are the front to rear vertical tire force ratio of left and right side of vehicle respectively. The equations (13), (14) and (19) can be rewritten as:

$$T_{m-fl}+T_{m-fr}+T_{m-rl}+T_{m-rr} = \frac{r_w}{n_g}F_{xd} \quad (19)$$

$$\frac{t_f}{2}T_{m-fr}-\frac{t_f}{2}T_{m-fl}+\frac{t_r}{2}T_{m-rr}-\frac{t_r}{2}T_{m-rl} = \frac{r_w}{n_g}M_{zd} \quad (20)$$

$$T_{m-fl}-\rho_L\,T_{m-rl} = 0 \quad (21)$$

$$T_{m-fr}-\rho_R\,T_{m-rr} = 0 \quad (22)$$

These equations can be expressed in matrix form and solved to obtain the command torques for the four in-wheel electric motor controllers.

4. Simulation Results

To verify the effectiveness of the proposed control algorithm, a lane-change maneuver on a slippery road was simulated using MATLAB/Simulink and CarSim. Since

optimal energy-efficient control allocation is especially critical when the EV requires large torque, the simulation focuses on a lane-change maneuver while the vehicle accelerates on a slippery road with a friction coefficient of 0.5. Vehicle and electric motor parameters are provided in Table 1.

Table 1
Vehicle and electric motor parameters

Parameter (unit)	Value	Parameter (unit)	Value	Parameter (unit)	Value
$m\,(kg)$	850	$r_w\,(m)$	0.26	$K_{us}\,(\frac{rad\,s^2}{m})$	0.004
$I_z\,(kgm^2)$	930	C_d	0.4	$T_{\max}\,(Nm)$	128
$a\,(m)$	0.81	$\rho_a\,(kg/m^3)$	1.206	$P_{\max}\,(kW)$	25
$b\,(m)$	0.99	$A_f\,(m^2)$	1.6	$L_s\,(H)$	0.003
$L\,(m)$	1.8	$t_f\,(m)$	1.415	$R_s\,(\Omega)$	0.3
$h_g\,(m)$	0.51	$t_r\,(m)$	1.375	n_g	2

The steering wheel angle applied by the driver is shown in Fig 5(a). Figs 5(b) to 5(e) display the longitudinal velocity, yaw rate, sideslip angle, and lateral acceleration of both the controlled and uncontrolled vehicles.

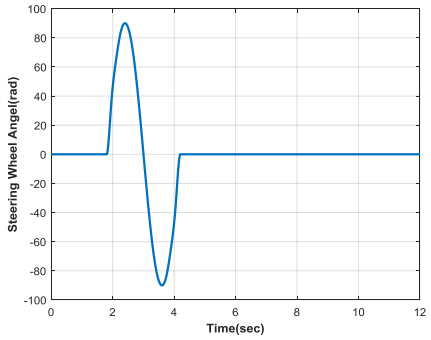

(a)

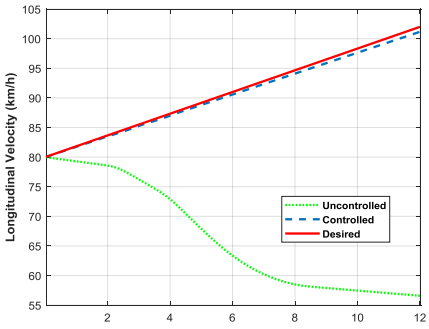

(b)

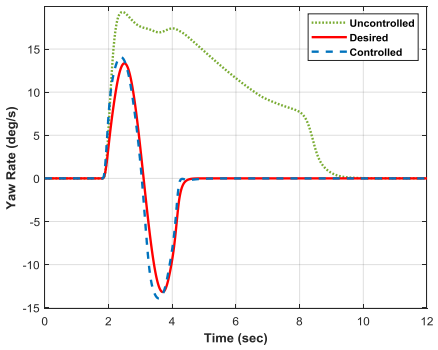

(c)

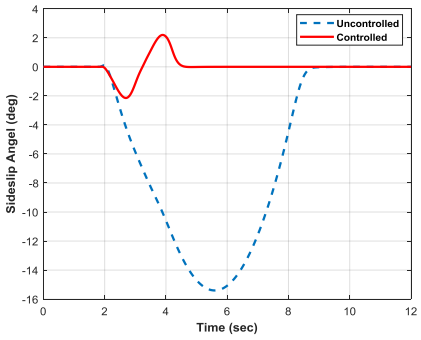

(d)

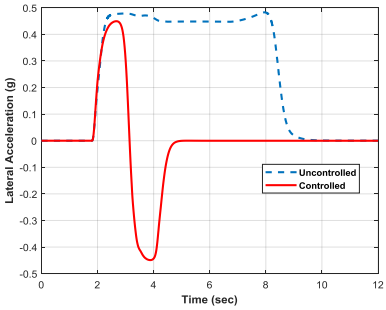

(e)

Fig 6. Simulation results in lane change maneuver on slippery road; (a) steering wheel angle (deg), (b) vehicle longitudinal velocity (km/h), (c) yaw rate (deg/s), (d) sideslip angle (deg), (e) lateral acceleration (g).

As shown in Fig 6(b), the longitudinal velocity of the controlled vehicle increases with a longitudinal acceleration of 0.1g, while the uncontrolled vehicle velocity decreases. This is because the sideslip angle of the uncontrolled vehicle increases rapidly during the lane change, as shown in Fig 6(d). The sideslip angle of the controlled vehicle remains small, ensuring that the vehicle performs the maneuver within a stable region. Fig 6(c) demonstrates that the controller successfully tracks the desired yaw rate during the lane change, while the uncontrolled vehicle deviates from the desired yaw rate and slides during the second half of the maneuver. Fig 6(e) shows that the lateral acceleration of the controlled vehicle closely matches the driver's steering input, while the uncontrolled vehicle lateral acceleration becomes saturated due to the low road friction coefficient.

4.1 Comparison of torque distribution algorithms

To compare the performance of the two torque distribution algorithms, the EV performs a double-lane-change maneuver while accelerating on a slippery road with a friction coefficient of 0.5. Figs 7(a) to 7(e) present a comparison of the yaw rate, sideslip angle, and torques of the front left and rear left motors for the two torque distribution algorithms. As seen in Figs 7(a) and 7(b), both controllers show similar performance in tracking the desired yaw rate and enhancing vehicle stability. However, Figs 7(c) and 7(d) reveal that the minimum power torque distribution algorithm allocates more torque to the front wheels compared to the dynamic load torque distribution algorithm. As a result, considering motor efficiency, the power consumption of the electric motors under the minimum power torque distribution is lower than that under the dynamic load torque distribution, as demonstrated in Fig 7(e).

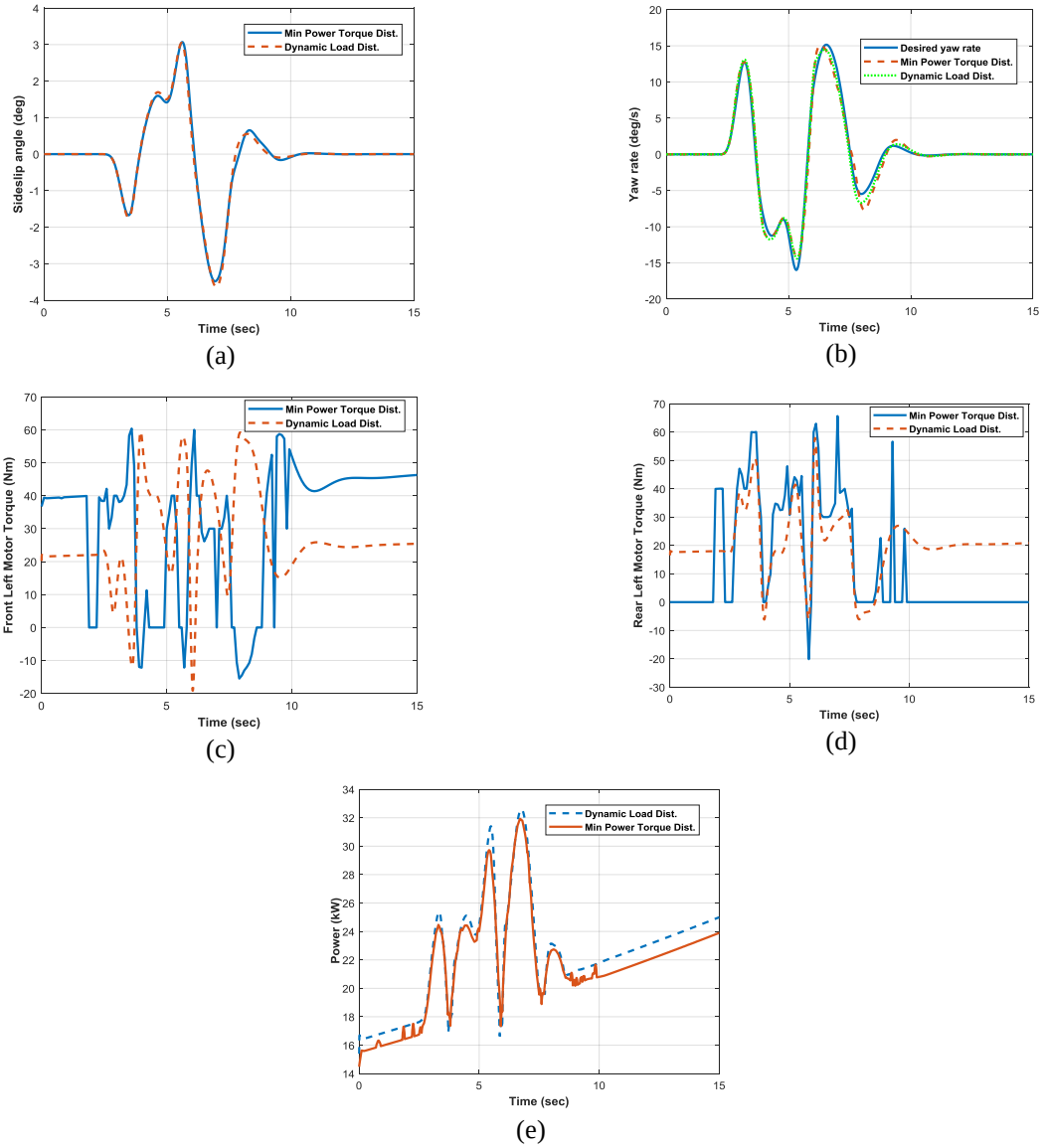

Fig 7. Vehicle simulation in double-lane change maneuver on slippery road; (a) sideslip angle (deg) (b) yaw rate (deg/s), (c) Front left motor torque (d) Rear left motor torque (c) motor power consumption comparison with two torque distribution algorithms.

5. Conclusion

An energy-efficient optimization allocation method for reducing power consumption in distributed EVs with equal drivetrains on the front and rear axles has been proposed for low-level controller operations during various maneuvers. At the high-level controller, the desired driving torque and yaw moment are determined using Sliding Mode Control (SMC). Additionally, energy regeneration, which contributes significantly to overall energy consumption, is also considered and should be fully utilized. Based on simulation results, the conclusion can be drawn that, under normal driving or braking conditions, the total torque should be evenly distributed across the four motors to minimize power consumption. Future control allocation algorithms should also consider other sources of energy dissipation, such as tire slip, which becomes particularly important at higher acceleration levels.

References

[1] D. Wang *et al.*, Review of Energy-Saving Technologies for Electric Vehicles, from the Perspective of Driving Energy Management, Sustainability, 15 (2023) 7617.

[2] A. Khajepour, M. S. Fallah, and A. Goodarzi, Electric and Hybrid Vehicles: Technologies, Modeling and Control-A Mechatronic Approach. John Wiley & Sons, 2014.

[3] B. Mashadi and M. Majidi, Integrated AFS/DYC sliding mode controller for a hybrid electric vehicle, International Journal of Vehicle Design, 56 (2011) 246-269.

[4] J. Park, H. Jeong, I. G. Jang, and S.-H. Hwang, Torque distribution algorithm for an independently driven electric vehicle using a fuzzy control method, Energies, 8 (2015) 8537-8561.

[5] A. M. Dizqah, B. Lenzo, A. Sorniotti, P. Gruber, S. Fallah, and J. De Smet, A fast and parametric torque distribution strategy for four-wheel-drive energy-efficient electric vehicles, IEEE Transactions on Industrial Electronics, 63 (2016) 4367-4376.

[6] S. Koehler, A. Viehl, O. Bringmann, and W. Rosenstiel, Energy-efficiency optimization of torque vectoring control for battery electric vehicles, IEEE Intelligent Transportation Systems Magazine, 9 (2017) 59-74.

[7] G. De Filippis, B. Lenzo, A. Sorniotti, P. Gruber, and W. De Nijs, Energy-efficient torque-vectoring control of electric vehicles with multiple drivetrains, IEEE Transactions on Vehicular Technology, 67 (2018) 4702-4715.

[8] W. Sun, J. Wang, Q. Wang, F. Assadian, and B. Fu, Simulation investigation of tractive energy conservation for a cornering rear-wheel-independent-drive electric vehicle through torque vectoring, Science China Technological Sciences, 61 (2018) 257-272.

[9] W. Xu, H. Chen, H. Zhao, and B. Ren, Torque optimization control for electric vehicles with four in-wheel motors equipped with regenerative braking system, Mechatronics, 57 (2019) 95-108.

[10] X. Hu, P. Wang, Y. Hu, and H. Chen, A stability-guaranteed and energy-conserving torque distribution strategy for electric vehicles under extreme conditions, Applied Energy, 259 (2020) 114162.

[11] X. Hu, H. Chen, Z. Li, and P. Wang, An energy-saving torque vectoring control strategy for electric vehicles considering handling stability under extreme conditions, IEEE Transactions on Vehicular Technology, 69 (2020) 10787-10796.

[12] S. H. Kim and K.-K. K. Kim, Model Predictive Control for Energy-efficient Yaw-stabilizing Torque Vectoring in Electric Vehicles with Four In-wheel Motors, IEEE Access, (2023).

[13] H. Deng, Y. Zhao, F. Lin, and Q. Wang, Deep Reinforcement Learning-Based Torque Vectoring Control Considering Economy and Safety, Machines, 11 (2023) 459.

[14] J. Wang, S. Gao, K. Wang, Y. Wang, and Q. Wang, Wheel torque distribution optimization of four-wheel independent-drive electric vehicle for energy efficient driving, Control Engineering Practice, 110 (2021) 104779.